

Comparative DNA Methylation Profiling Reveals an Immunoepigenetic Signature of HIV-related Cognitive Impairment

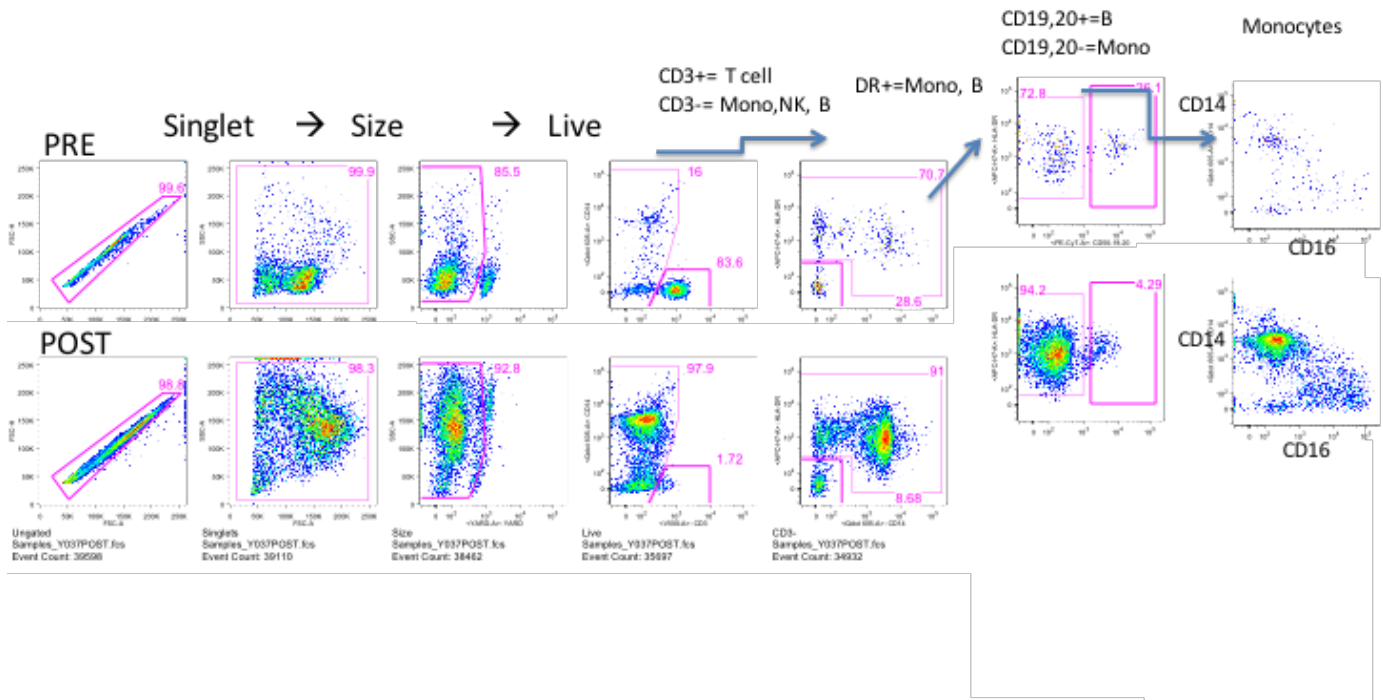
Michael J. Corley¹, Christian Dye¹, Michelle D'Antoni Brogan², Mary Margaret Byron², Kaahukane Leite-Ah Yo¹, Annette Lum-Jones¹, Beau Nakamoto³, Victor Valcour⁴, Ivo Sah Bandar², Cecilia M. Shikuma³, *Lishomwa C. Ndhlovu^{2,3}, and *Alika K. Maunakea¹

¹Department of Native Hawaiian Health, John A. Burns School of Medicine, Suite 1016B, University of Hawaii, Honolulu, HI 96813, USA.

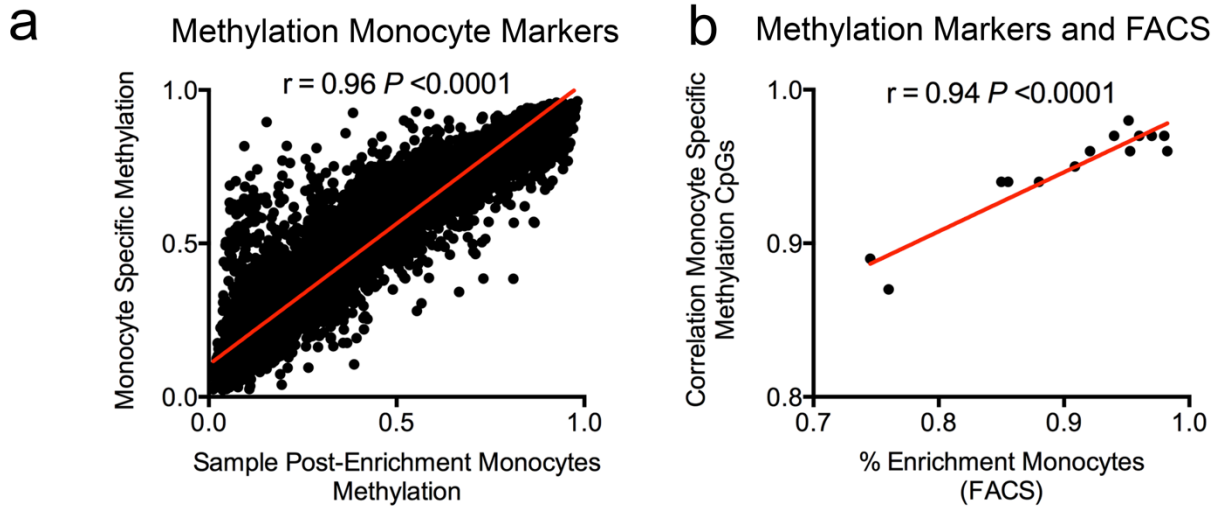
²Department of Tropical Medicine, ³Hawaii Center for AIDS, John A. Burns School of Medicine, University of Hawaii, 651 Ilalo Street, BSB, Honolulu, HI 96815, USA,

⁴Memory and Aging Center, Department of Neurology, University of California, San Francisco, CA, USA

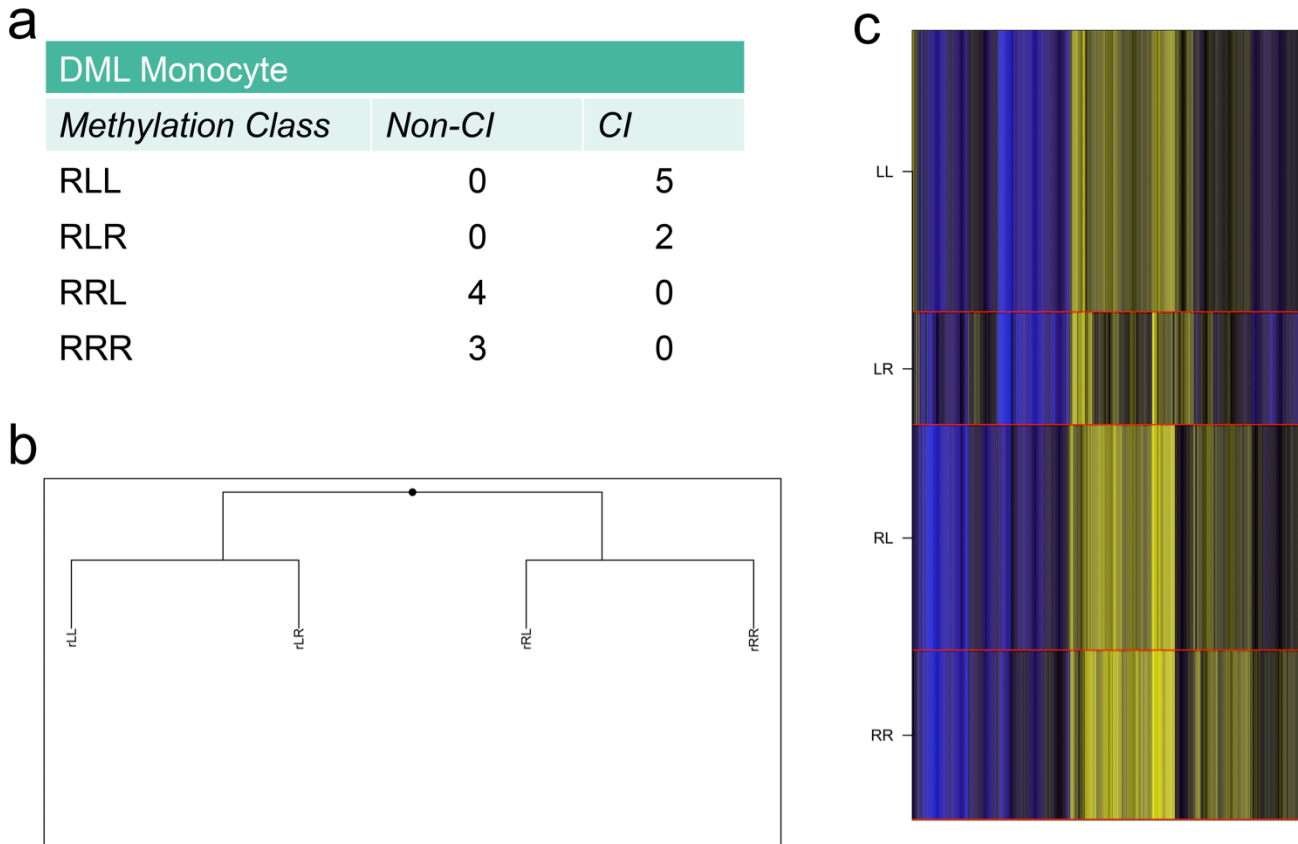
Supplementary Information



Supplementary Figure S1. Gating Strategy to confirm monocyte enrichment post-immunomagnetic enrichment. Aliquots of pre- (Top row) and post-immunomagnetic (Bottom row) negative selection enrichment PBMCs were analyzed for percent CD14(+)CD16(+) monocytes based on gating strategies previously described¹.

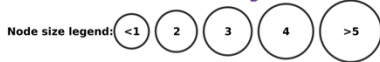


Supplementary Figure S2. Validation of monocyte cell enrichment by cell type-specific DNA methylation analysis. (a) Relationship between reference DNA methylation dataset for monocyte cell type and Post-enrichment DNA methylation for study sample. **(b)** Relationship between correlation based on monocyte cell-type specific analysis and % enrichment monocytes calculated by FACS analysis.



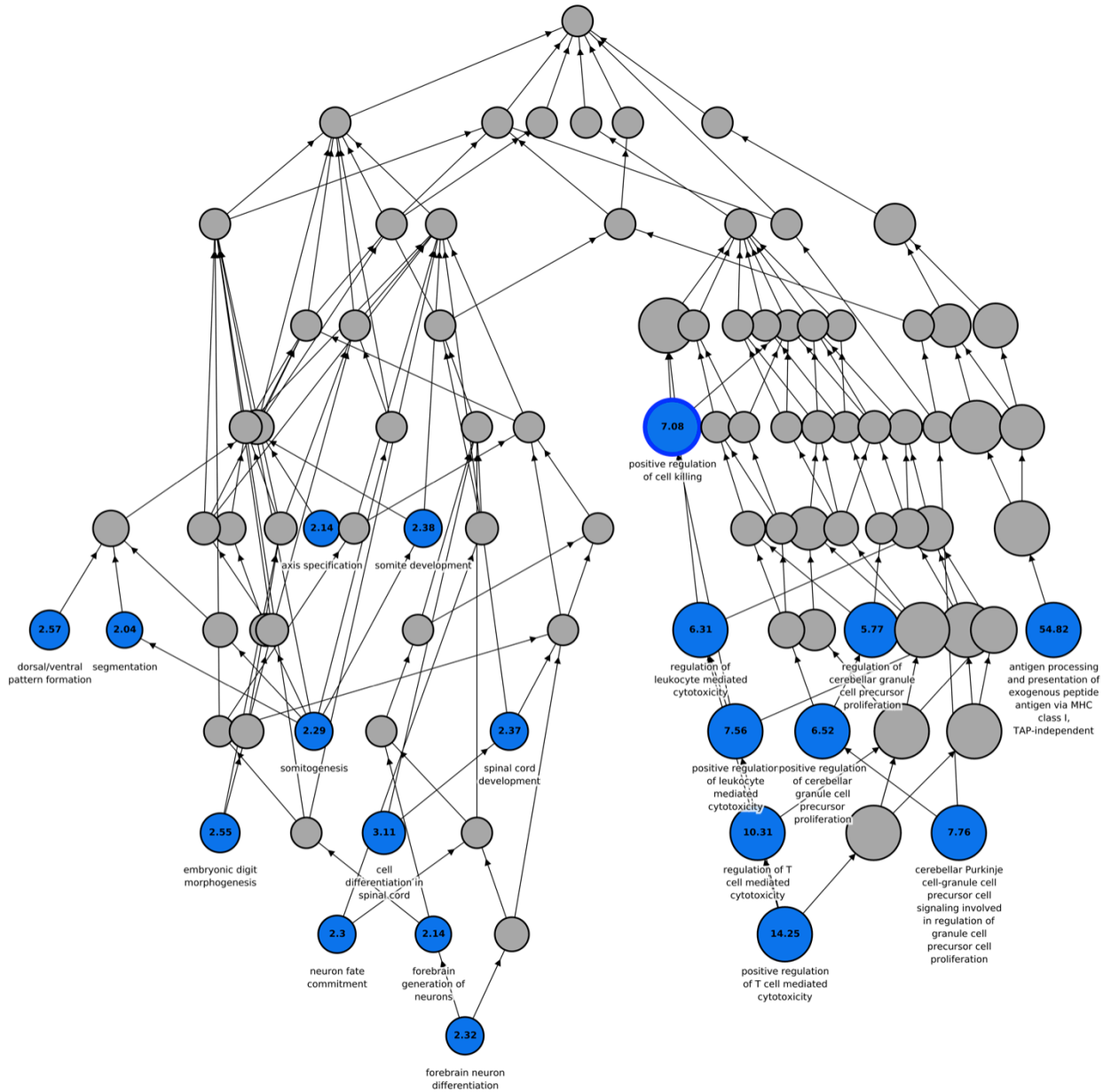
Supplementary Figure S3. Clustering of Differentially Methylated Loci in Monocytes with recursively partitioned mixture modeling (RPMM). (a) Methylation profile classes from RPMM of monocyte DML from Non-CI and CI participants. (b) RPMM tree dendrogram showing 4 methylation classes clustering Non-CI and CI participants. (c) Columns represent differentially methylated CpG sites and rows represent the methylation classes. Row height displays number of observations residing in the class and red lines separates methylation classes. Blue indicates methylated and yellow indicates unmethylated.

Monocytes



Local DAG for enriched terms in GO Biological Process

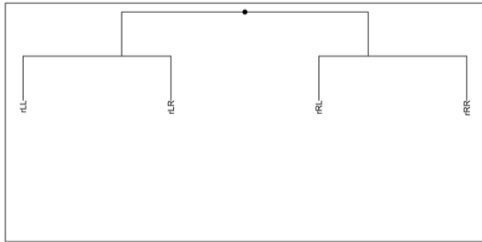
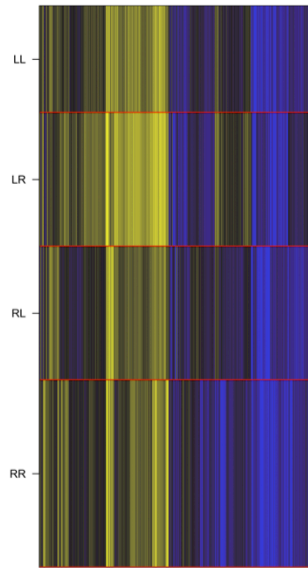
Nodes sized according to Binomial Fold Enrichment



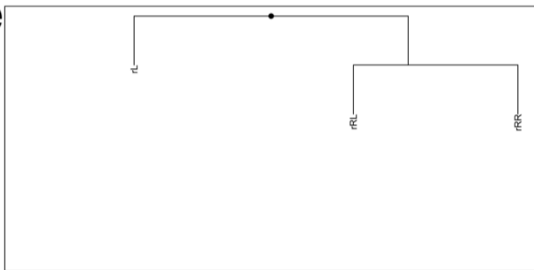
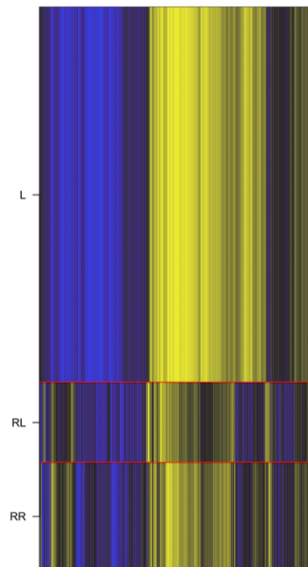
Supplementary Figure S4. GREAT analysis Gene Ontology Enrichment for Differentially Methylated Loci in Monocytes. HIV-associated cognitively impaired differentially methylated loci identified in monocytes were converted to genomic positions and analyzed using the GREAT tool². Binomial fold enrichment presented in each node and enriched nodes term presented below.

a

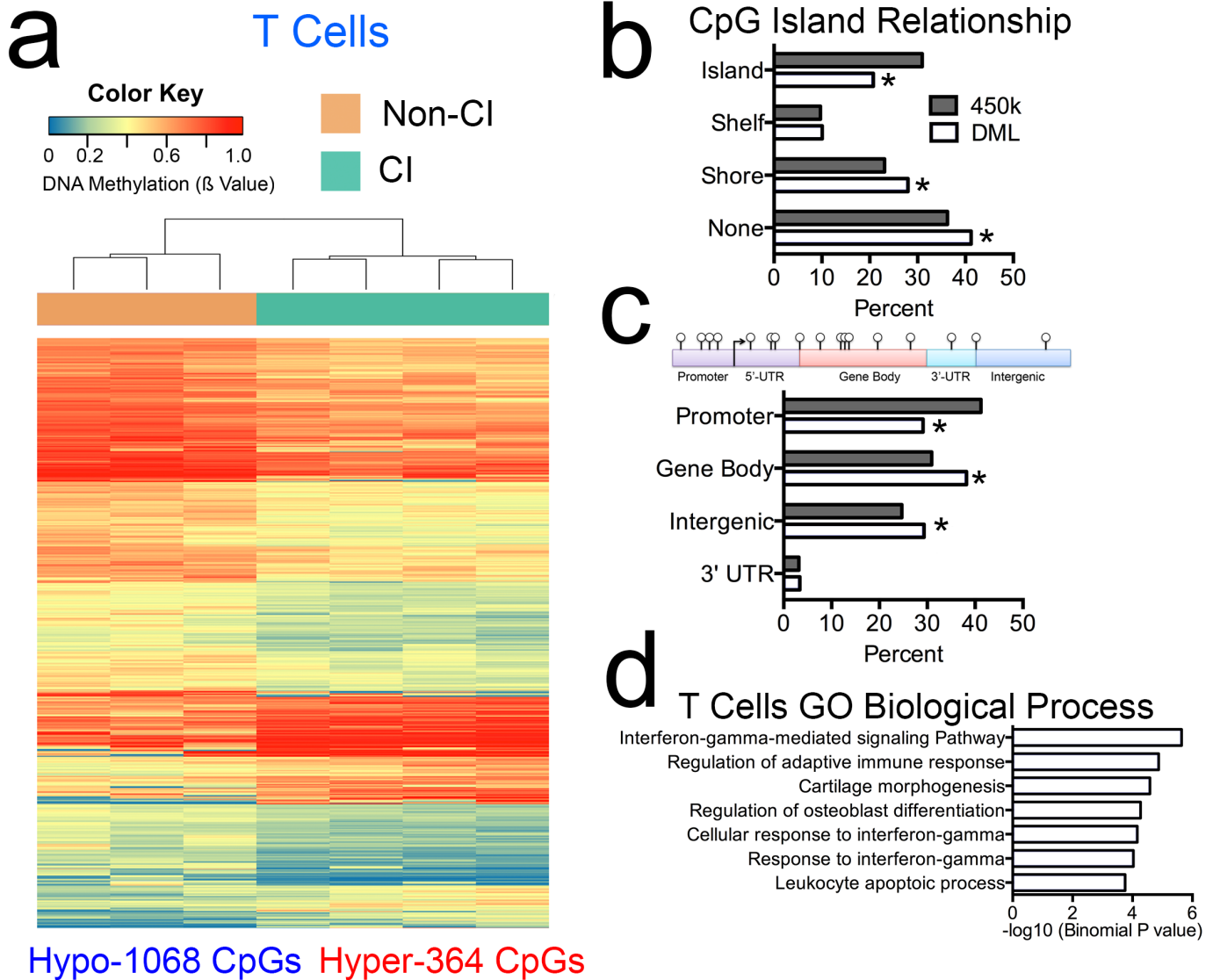
| DML Monocyte Profile | | | | |
|----------------------|----------|----|--------|----|
| Methylation Class | Monocyte | | T Cell | |
| | Non-CI | CI | Non-CI | CI |
| RLL | 2 | 2 | 0 | 0 |
| RLR | 0 | 5 | 0 | 0 |
| RRL | 5 | 0 | 0 | 0 |
| RRR | 0 | 0 | 3 | 4 |

b**c****d**

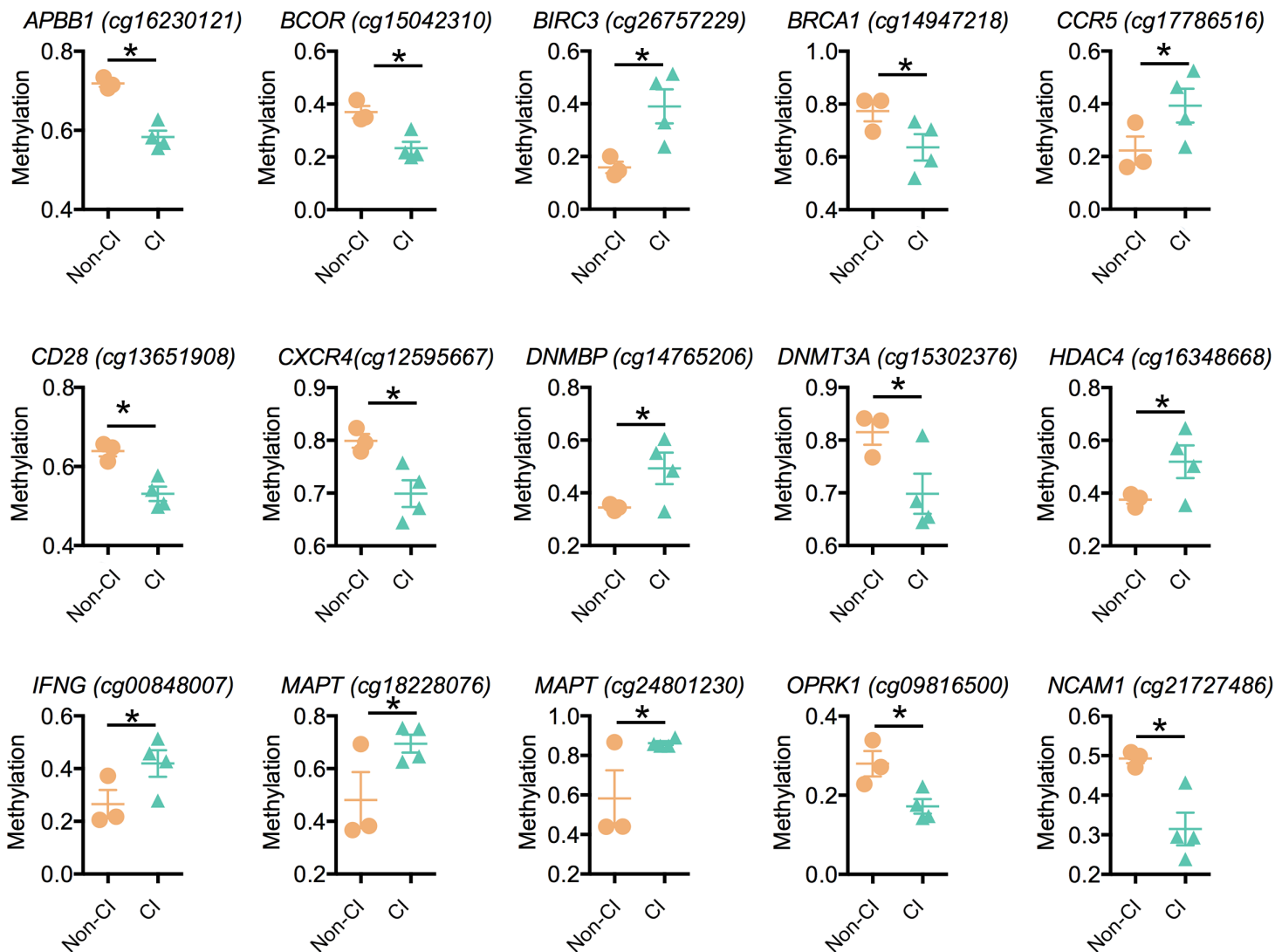
| DML T Cell Profile | | | | |
|--------------------|----------|----|--------|----|
| Methylation Class | Monocyte | | T Cell | |
| | Non-CI | CI | Non-CI | CI |
| RL | 7 | 7 | 0 | 0 |
| RRL | 0 | 0 | 3 | 0 |
| RRR | 0 | 0 | 0 | 4 |

e**f**

Supplementary Figure S5. CI-associated DML in monocytes stratifies CI in T cells with recursively partitioned mixture modeling (RPMM). (a) Methylation profile classes from RPMM analysis of monocyte DML profile from Non-CI and CI participants monocytes and T cells. (b) RPMM tree dendrogram showing 4 methylation classes clustering Non-CI and CI participants. (c) Columns represent differentially methylated CpG sites and rows represent the methylation classes. Row height displays number of observations residing in the class and red lines separates methylation classes. Blue indicates methylated and yellow indicates unmethylated. (d) Methylation profile classes from RPMM analysis of CD8+ T Cell DML profile from Non-CI and CI participants monocytes and T cells. (e) RPMM tree dendrogram showing 4 methylation classes clustering Non-CI and CI participants. (f) Columns represent differentially methylated CpG sites and rows represent the methylation classes. Row height displays number of observations residing in the class and red lines separates methylation classes. Blue indicates methylated and yellow indicates unmethylated.



Supplementary Figure S6. HIV CI-associated DNA methylation differences in CD8+ T cells. (a) Heatmap displaying methylation levels of differentially methylated loci in Non-CI (orange) and CI (green) monocyte samples. The majority of these loci were hypo-methylated in CI compared to Non-CI. Unsupervised hierarchical clustering analysis (Manhattan distance, complete linkage method) above columns stratifies Non-CI and CI samples. Methylation values of each CpG displayed ranging from low methylation (0, blue) to high methylation (1, red). (b) Plot showing percent differentially methylated loci (white) located in CpG islands, shelves, shores, or none (Non-CpG island) compared to percent observed for all probes on the 450k array (grey). Significant enrichment for DML in CpG island shores compared to expected by chance. (c) Percent differentially methylated loci (white) located in gene promoters, gene bodies, intergenic regions, and 3' UTR compared to percent observed for all probes on the 450k array (grey) shows significantly higher than expected gene body and intergenic location of loci compared to expected by chance. (d) GREAT analysis of DML displaying significant GO biological processes.



Supplementary Figure S7. HIV CI-associated DNA methylation differences in CD8+ T cells.

Differentially methylated loci in Non-CI and CI T cell samples located in genes related to central nervous system, interactions with HIV, and epigenetic mechanisms. * $P < 0.05$

Supplemental Table S1. Cognitive Impaired (CI) and Non-CI Samples

| Group | PID | Cognition |
|---------------|------------|------------------|
| <i>Non-CI</i> | Y041S | Normal |
| | Y135S | Normal |
| | Y136C | Normal |
| | Y160L | Normal |
| | Y068 | Normal |
| | Y078 | Normal |
| | Y106 | Normal |
| | Y028 | Normal |
| | Y065 | Normal |
| | Y103 | Normal |
| <i>CI</i> | Y168Z | HAD |
| | Y211T | HAD |
| | Y213P | MC/MD |
| | Y037 | MC/MD |
| | Y060 | HAD |
| | Y113 | MC/MD |
| | Y008 | MC/MD |
| | Y082 | MC/MD |
| | Y094 | HAD |
| | Y105 | HAD |
| | Y118 | HAD |

Supplemental Table S2. FACS cell frequency percent following CD14+CD16+ monocyte enrichment

| Non-CI | | Pre-Enrichment | | | | | Post-Enrichment | | | | | Monocyte Methylation Correlation |
|-----------|----------------|----------------|-----------------------|--------|--------|---------|------------------------|-------|--------|--------|---------|----------------------------------|
| PID | Log Viral Load | Cell Count | Mono | T Cell | B Cell | NK Cell | Cell Count | Mono | T Cell | B Cell | NK Cell | |
| Y041S | 1.68 | 13 M | 24.4% | 63.3% | 3.1% | 9.3% | 2.25 M | 93.9% | 0.2% | 0.4% | 5.6% | 0.97 |
| Y136C | 4.08 | 15 M | 29.7% | 64.9% | 1.8% | 3.7% | 2.5 M | 98.4% | 0.4% | 0.3% | 1.0% | 0.97 |
| Y160L | 1.68 | 4.7 M | 10.6% | 84.3% | 2.0% | 3.1% | 550 K | 97.4% | 0.2% | 0.7% | 1.8% | 0.97 |
| Y068 | 3.56 | 4.4 M | 12.4% | 79.2% | 4.0% | 4.5% | 800 K | 85.1% | 3.1% | 6.6% | 5.3% | 0.94 |
| Y106 | 4.09 | 4.9 M | 41.7% | 39.2% | 11.9% | 7.2% | 600 K | 76.0% | 7.7% | 11.3% | 5.0% | 0.87 |
| Y135S | 2.25 | 9.6 M | 20.2% | 69.2% | 2.3% | 8.3% | 800 K | 95.9% | 0.1% | 0.5% | 3.4% | 0.97 |
| Y078 | 1.69 | 6.6 M | 6.0% | 85.1% | 4.6% | 4.4% | 525 K | 88.1% | 3.3% | 5.1% | 3.5% | 0.94 |
| Mean | | | 20.7% | 69.3% | 4.2% | 5.8% | | 90.7% | 2.1% | 3.6% | 3.7% | |
| CI | | | Pre-Enrichment | | | | Post-Enrichment | | | | | |
| Y168Z | 1.68 | 22 M | 15.0% | 76.6% | 3.0% | 5.4% | 2.45 M | 92.1% | 1.6% | 1.3% | 5.1% | 0.96 |
| Y211T | 1.68 | 5.7 M | 15.6% | 73.9% | 3.3% | 7.2% | 950 K | 95.3% | 1.2% | 0.6% | 2.9% | 0.96 |
| Y213 | 1.68 | 6.1 M | 24.4% | 67.7% | 0.9% | 7.0% | 1.2 M | 95.2% | 0.1% | 0.5% | 4.3% | 0.98 |
| Y060 | 2.96 | 6.3 M | 10.7% | 80.9% | 0.9% | 2.8% | 825 K | 90.9% | 2.4% | 4.9% | 1.8% | 0.95 |
| Y113 | 1.69 | 6.9 M | 12.8% | 77.7% | 5.8% | 3.8% | 625 K | 85.6% | 0.8% | 4.0% | 9.6% | 0.94 |
| Y037 | 1.69 | 14 M | 14.3% | 78.0% | 3.2% | 4.5% | 1.8 M | 98.2% | 0.1% | 0.2% | 1.5% | 0.96 |
| Y008 | 1.69 | 2.2 M | 17.9% | 60.8% | 2.0% | 7.9% | 450 K | 74.5% | 9.4% | 11.5% | 4.6% | 0.89 |
| Mean | | | 15.8% | 73.7% | 2.7% | 5.5% | | 90.3% | 2.2% | 3.3% | 4.3% | |

Supplemental Table S3. Enrichr Gene List Analysis: GO Biological Process

| Name | P-value | Combined Score |
|--|----------------|-----------------------|
| regulation of ion transmembrane transport (GO:0034765) | 2.51E-07 | 18.0 |
| regulation of transmembrane transport (GO:0034762) | 5.19E-07 | 18.0 |
| homophilic cell adhesion via plasma membrane adhesion molecules (GO:0007156) | 3.24E-07 | 16.9 |
| cell-cell adhesion (GO:0098609) | 8.95E-07 | 16.7 |
| cell-cell adhesion via plasma-membrane adhesion molecules (GO:0098742) | 8.32E-07 | 16.7 |
| single-organism behavior (GO:0044708) | 8.97E-06 | 13.0 |
| behavior (GO:0007610) | 1.25E-05 | 12.6 |
| neuron recognition (GO:0008038) | 4.39E-05 | 10.8 |
| locomotory behavior (GO:0007626) | 2.89E-05 | 10.6 |
| regulation of appetite (GO:0032098) | 1.93E-04 | 8.2 |
| adult behavior (GO:0030534) | 9.83E-05 | 8.1 |
| regulation of endothelial cell proliferation (GO:0001936) | 1.32E-04 | 7.6 |
| regulation of calcium ion transport (GO:0051924) | 1.72E-04 | 7.6 |
| positive regulation of cell projection organization (GO:0031346) | 1.93E-04 | 7.3 |
| regionalization (GO:0003002) | 2.56E-04 | 7.2 |
| cognition (GO:0050890) | 3.01E-04 | 6.8 |
| neuron migration (GO:0001764) | 2.67E-04 | 6.6 |
| pattern specification process (GO:0007389) | 4.06E-04 | 6.4 |
| positive regulation of calcium-mediated signaling (GO:0050850) | 7.10E-04 | 5.8 |
| regulation of metal ion transport (GO:0010959) | 8.10E-04 | 5.6 |

Supplemental Table S4. Enrichr Gene List Analysis: GO Cellular Component

| Name | P-value | Combined Score |
|--|----------------|-----------------------|
| synapse part (GO:0044456) | 1.95E-05 | 12.0 |
| ion channel complex (GO:0034702) | 2.73E-04 | 8.0 |
| extracellular matrix (GO:0031012) | 1.70E-04 | 8.0 |
| synapse (GO:0045202) | 4.14E-04 | 7.9 |
| synaptic vesicle (GO:0008021) | 3.85E-04 | 7.8 |
| transmembrane transporter complex (GO:1902495) | 8.24E-04 | 7.1 |
| transporter complex (GO:1990351) | 9.87E-04 | 7.0 |
| integral component of plasma membrane (GO:0005887) | 7.32E-04 | 6.8 |
| anchored component of membrane (GO:0031225) | 1.46E-03 | 5.8 |
| external side of plasma membrane (GO:0009897) | 3.07E-03 | 5.2 |
| proteinaceous extracellular matrix (GO:0005578) | 2.64E-03 | 5.0 |
| terminal bouton (GO:0043195) | 3.53E-03 | 4.8 |
| side of membrane (GO:0098552) | 5.81E-03 | 4.3 |
| axon part (GO:0033267) | 6.30E-03 | 4.0 |
| photoreceptor inner segment (GO:0001917) | 5.03E-03 | 4.0 |
| synaptic membrane (GO:0097060) | 1.12E-02 | 3.5 |
| collagen trimer (GO:0005581) | 8.21E-03 | 3.5 |
| cell surface (GO:0009986) | 1.13E-02 | 3.4 |
| perikaryon (GO:0043204) | 7.87E-03 | 3.4 |
| cation channel complex (GO:0034703) | 1.13E-02 | 3.2 |

Supplemental Table S5. Enrichr Gene List Analysis: GO Molecular Function

| Name | P-value | Combined Score |
|---|----------------|-----------------------|
| sulfur compound binding (GO:1901681) | 3.92E-05 | 8.8 |
| carboxylic acid binding (GO:0031406) | 2.95E-04 | 6.8 |
| organic acid binding (GO:0043177) | 3.10E-04 | 6.8 |
| calcium ion binding (GO:0005509) | 5.91E-04 | 5.7 |
| transforming growth factor beta binding (GO:0050431) | 1.29E-03 | 5.5 |
| structural constituent of muscle (GO:0008307) | 9.92E-04 | 5.2 |
| substrate-specific channel activity (GO:0022838) | 2.16E-03 | 4.9 |
| cell adhesion molecule binding (GO:0050839) | 1.72E-03 | 4.7 |
| passive transmembrane transporter activity (GO:0022803) | 3.80E-03 | 4.6 |
| channel activity (GO:0015267) | 3.80E-03 | 4.6 |
| transmembrane receptor protein kinase activity (GO:0019199) | 1.70E-03 | 4.5 |
| amino acid binding (GO:0016597) | 2.31E-03 | 4.4 |
| gated channel activity (GO:0022836) | 4.72E-03 | 4.3 |
| voltage-gated ion channel activity (GO:0005244) | 4.27E-03 | 4.3 |
| voltage-gated channel activity (GO:0022832) | 4.27E-03 | 4.3 |
| glycosaminoglycan binding (GO:0005539) | 4.44E-03 | 4.1 |
| neurotransmitter receptor activity (GO:0030594) | 3.83E-03 | 4.0 |
| phosphoric ester hydrolase activity (GO:0042578) | 6.09E-03 | 4.0 |
| heparin binding (GO:0008201) | 4.08E-03 | 4.0 |
| ion channel activity (GO:0005216) | 7.38E-03 | 3.9 |

Supplemental Table S6. Monocyte DML: Loci Related to Inflammatory Response

Monocytes DMS: Inflammatory Response

| Probe ID | Genomic Position | Gene | Gene Region | P-value | Mean CI | Mean Non-CI | Beta Diff. |
|------------|--------------------------|---------------|-------------|---------|---------|-------------|------------|
| cg24491749 | chr4:107236485-107236486 | <i>AIMP1</i> | TSS1500 | 0.01 | 0.48 | 0.64 | 0.16 |
| cg00887153 | chr16:71559593-71559594 | <i>CHST4</i> | TSS1500 | 0.04 | 0.59 | 0.48 | 0.11 |
| cg01360628 | chr3:89156118-89156119 | <i>EPHA3</i> | TSS1500 | 0.05 | 0.61 | 0.49 | 0.12 |
| cg05463589 | chr16:88706426-88706427 | <i>IL17C</i> | Body | 0.01 | 0.65 | 0.46 | 0.19 |
| cg21593409 | chr16:88706389-88706390 | <i>IL17C</i> | Body | 0.01 | 0.62 | 0.48 | 0.14 |
| cg11931596 | chr8:79674645-79674646 | <i>IL7</i> | Body | 0.04 | 0.38 | 0.27 | 0.11 |
| cg12454167 | chr3:186435060-186435061 | <i>KNG1</i> | TSS200 | 0.01 | 0.77 | 0.64 | 0.13 |
| cg13150801 | chr6:6606065-6606066 | <i>LY86</i> | Body | 0.02 | 0.59 | 0.46 | 0.13 |
| cg06823034 | chr14:24780734-24780735 | <i>LTB4R</i> | 5'UTR | 0.01 | 0.19 | 0.09 | 0.11 |
| cg00831909 | chr1:13909623-13909624 | <i>PDPN</i> | TSS1500 | 0.02 | 0.56 | 0.44 | 0.13 |
| cg19702271 | chr6:46703495-46703496 | <i>PLA2G7</i> | TSS1500 | 0.00 | 0.31 | 0.20 | 0.11 |
| cg25503381 | chr15:39871923-39871924 | <i>THBS1</i> | TSS1500 | 0.01 | 0.77 | 0.89 | 0.12 |
| cg08433504 | chr15:39872071-39872072 | <i>THBS1</i> | TSS1500 | 0.02 | 0.75 | 0.87 | 0.12 |
| cg10078511 | chr15:39872032-39872033 | <i>THBS1</i> | TSS1500 | 0.02 | 0.73 | 0.83 | 0.10 |
| cg26123256 | chr2:27530670-27530671 | <i>UCN</i> | Body | 0.02 | 0.45 | 0.35 | 0.10 |

Supplemental Table S7. Cytokine Signaling in Immune System Genes Differentially Expressed between CI and Non-CI Monocytes

| Gene Symbol | Mean RPM Non-CI | Mean RPM CI | P-value |
|--------------------|----------------------------|------------------------|----------------|
| <i>CISH</i> | 29.84 | 14.20 | 1.37E-03 |
| <i>DDX58</i> | 105.69 | 54.01 | 3.75E-02 |
| <i>EGR1</i> | 888.81 | 1371.58 | 3.29E-02 |
| <i>HLA-F</i> | 29.68 | 15.26 | 2.64E-02 |
| <i>IFIT1</i> | 42.70 | 12.14 | 1.39E-02 |
| <i>IFIT2</i> | 164.80 | 65.84 | 2.29E-02 |
| <i>IFIT3</i> | 112.37 | 37.18 | 9.49E-03 |
| <i>IL1B</i> | 36.37 | 144.39 | 1.66E-02 |
| <i>IL2RB</i> | 53.62 | 25.95 | 3.38E-02 |
| <i>IRS2</i> | 73.33 | 138.86 | 1.76E-02 |
| <i>JAK3</i> | 215.10 | 139.92 | 4.54E-02 |
| <i>NR4A2</i> | 13.30 | 52.68 | 1.18E-04 |
| <i>NUP50</i> | 72.35 | 46.56 | 2.32E-02 |
| <i>OAS2</i> | 171.45 | 81.92 | 2.25E-02 |
| <i>OAS3</i> | 453.95 | 215.73 | 4.67E-02 |
| <i>PELI1</i> | 82.05 | 169.82 | 5.45E-03 |
| <i>RIPK2</i> | 62.47 | 119.02 | 7.09E-03 |
| <i>RSAD2</i> | 39.80 | 11.54 | 1.33E-02 |
| <i>STAT2</i> | 597.09 | 343.93 | 1.03E-02 |
| <i>TRIM21</i> | 48.64 | 28.57 | 2.89E-02 |
| <i>TRIM26</i> | 53.82 | 36.53 | 4.79E-02 |
| <i>UBE2E1</i> | 45.47 | 23.77 | 1.17E-02 |

Supplemental Table S8. Cell Type Specific DNA Methylation T Cell Enrichment Analysis Results

| Non-CI | T Cell Methylation Correlation |
|---------------|---------------------------------------|
| Y028 | 0.89 |
| Y065 | 0.86 |
| Y103 | 0.89 |

| CI | |
|-----------|------|
| Y082 | 0.93 |
| Y094 | 0.93 |
| Y105 | 0.90 |
| Y118 | 0.92 |

Supplementary References

- 1 Ndhlovu, L. C. *et al.* Loss of CCR2 expressing non-classical monocytes are associated with cognitive impairment in antiretroviral therapy-naive HIV-infected Thais. *Journal of neuroimmunology* **288**, 25-33, doi:10.1016/j.jneuroim.2015.08.020 (2015).
- 2 McLean, C. Y. *et al.* GREAT improves functional interpretation of cis-regulatory regions. *Nature biotechnology* **28**, 495-501, doi:10.1038/nbt.1630 (2010).